Geological storage of CO_2: heterogeneity impact on pressure behavior

October 28, 2013

Abstract

Due to the high rates of industrial CO_2 emission, it is an operational objective to maximize CO_2 injection rates into underground geological formations. Forcing high volumetric rates into the injection wells can result in an over-pressurized system, which can cause possible breakings in the formation integrity and can increase the risk of CO_2 leakage.

The goal of this study is to investigate the injection pressure considerations that are needed to avoid the uncontrolled development of fractures in the medium. Herein, we study how geological heterogeneity influences the pressure behavior of a typical CO_2 injection operation. Five geological feature variables are considered as inputs for the sensitivity analysis. These features include various levels of faults, lobosity, flow barriers, aggradation angle, and progradation direction.

Two injection scenarios are examined. In the first scenario, CO_2 is injected through a single well at a constant rate and the pressure in the well and the domain is allowed to build up without limit. In the second scenario, a pressure constraint is set on the well and the injection rate is changed to keep the pressure below the limit. Model responses related to pressure build-up and propagation within the system are defined and demonstrated using a selected case. Results for all cases are presented and discussed accordingly. We conclude by ranking aggradation angle, progradation direction, and faults as the most influential geological parameters.

The novelty of this work is in the extensive geological realizations and the introduced methods to analyze the pressure within the medium. The demonstrated work flow can be used in any extensive pressure study. The rankings of geological parameters based on their influence may change by selecting a larger model size or different injection scenarios, injection locations, or number of injectors.

1 Introduction

The industrial CO_2 emission rate is expected to increase over the next decade if necessary preventive actions are not taken. For example, according to the Energy Information Administration, carbon dioxide emissions in the United States are forecast to reach 6.41 billion

tonnes by 2030. The Kyoto Protocol proposed an emission cut that requires a reduction of 1.75 billion tonnes of carbon dioxide [15].

Geological storage of CO_2 is a proposed solution to fight global climate change. Clear operational criteria and policies must be made to avert unwanted consequences. Concerns connected to putting a large mass of CO_2 into underground geological formations are not limited to the spatial distribution of the injected fluid. The pressure signals imposed through the injection point can travel beyond the scale of the zones where CO_2 is present. Although geological barriers can hinder the pressure exchange between different regions, pressure can transfer through low-permeable rocks where the CO_2 is trapped by capillarity.

In addition to the depleted oil and gas fields, deep geological aquifers are practical targets for the geological storage of CO_2. If one is injecting into brine aquifers, the pressure waves can push the brine into connected fresh water aquifers, contaminating them. Brine displacement issues are discussed in [5] by defining open, closed, and semi-closed aquifer boundaries. Brine might also leak through abandoned wells into other zones. Cailly et al. [4] discuss well design considerations to prevent any leakage through wells.

Geomechanical deformations are important during the injection period. They can lead to changes in effective permeability and porosity. It is possible that the pressure build-up around injection wells can crack the rock with uncontrolled fractures extending to the structural sealing layers. Faults can be activated due to high pressure in the system, providing a leakage path across layers. In addition to the increased spatial spread of CO_2, an intensive induced fracture network can result in local earthquakes.

Pressure constraints must be considered for injection operations to limit the pressure build-up. However, this comes with the cost of injection rate reduction. Rock quality within the injection region has a significant impact on pressure build-up and therefore geological uncertainty plays a considerable role in assessing the success and feasibility of the operation.

Geological uncertainty is a major issue in pressure analysis. Most of the pressure-related studies in the literature provide either deterministic case studies or generic preventive measures based on theoretical studies [12, 16, 8, 17, 14, 13]. It is important to include realistic geological descriptions in any geological uncertainty study. For example, permeability variation in the grid should be included in the form of realizations of geological realistic formations. To the best of our knowledge, this is the first pressure study in the context of CO_2 storage that considers the geological uncertainty in the form of structural and sedimentological variables.

Within the context of oil recovery, the impact of geological uncertainty is thoroughly investigated in the SAIGUP project for shallow marine depositional systems [7, 9, 10]. In the SAIGUP study, variations of geological features are examined in a set of field development strategies via several injection/production patterns. The study concludes that geological uncertainty has a dramatic influence on the oil recovery estimates. A number of geological realizations from the SAIGUP project are used in [1, 2] to investigate the impact of geological uncertainty on the injection and early migration of CO_2. The focus in these studies is to measure the sensitivity of the spatial CO_2 distribution to the variation of the geological description. Certain structural features are considered for those studies and flow responses are defined to measure the storage capacity, the trapping efficiency, and the leakage risk. The sensitivity of these responses to variations in geological parameters is investigated. The results show large variation in responses. Aggradation angle and barriers are found to be the most influential in the CO_2 flow behavior [1, 2].

Simplified geological assumptions allow the use of established analytical solution of the flow governing equations. Neuman and Witherspoon [11] presented solutions that are useful for determining the hydrolic properties of leaky confined aquifer systems. They assumed that the aquifer is homogeneous, isotropic, and of uniform thickness. Moreover, they assumed the extents of the aquifer to be infinite. Chabora and Benson [6] used the analytical solution provided in [11] to study the leakage of the stored CO_2 through the cap-rock by measuring the pressure build-up in the aquifer. They performed sensitivity analysis on the pressure variation by changing the formation parameters and injection criteria. Chabora and Benson found a correlation between the pressure build-up values in the medium and the specifications of aquifer and injection operations. This correlation gives insight in the design and monitoring phases of the storage operations. Such pressure monitoring approaches are based on geological simplifications.

Injection causes pressure evolution in the domain that starts by transient pressure build-up near the injector. As the injection proceeds, the injected CO_2 invades larger region in the domain. The two phase region grows in size and the injected CO_2 moves in both vertical and horizontal directions within the aquifer. In the vertical direction, the CO_2 moves upward due to the buoyancy forces and in the horizontal direction, the influx from the injector pushes the CO_2 through the two phase zone. When the pressure pulse imposed by the injector reaches the boundaries of the domain, the average pressure in the aquifer increases in a quasi-steady state trend. Pressure build-up development in the medium, in particular the transient pressure changes, can be influenced dramatically by geological heterogeneities. This study aims to evaluate the importance of sophisticated geological modeling in simulating the pressure variation in the domain.

We perform detailed pressure analysis by simulating the flow within the SAIGUP geological setup. Our study demonstrates the value of realistic geological modeling in designing CO_2 storage operations and monitoring the pressure development in the aquifer.

Spatial pressure distribution in the aquifer depends on the domain extents. The available volume for CO_2 storage in closed or semi-closed systems with limited domain extents is mostly provided by medium compressibility in response to formation pressure build-up. Moreover, the cap-rock and structural traps that are supposed to be sealing allow the CO_2 to leak with a rate that depends to the pressure build-up in the aquifer.

Birkholzer et al. [3] investigated the influence of domain size on pressure rise in the medium due to CO_2 injection. They assumed homogeneous aquifer to study the pressure development in various model sizes, ranging from 10 to 100 km. They simulated CO_2 injection over 30 years in 250 m of formation with a rate of 120 kg/s. They performed sensitivity analysis with focus on the plume migration and the evolution of pressure build-up in the aquifer. In addition to the model extent, various hydrological properties are examined in [3] to study the impact on CO_2 storage capacity.

The results in [3] suggest that the storage capacity in closed and semi-closed aquifers is controlled by the operational pressure constraints and it is much smaller than the capacity of large aquifers.

The simulation results in [3] show that the region of evaluated pressure is much larger than the CO_2 plume size. In the model with 20 km domain extent, a substantial pressure increase from hydrostatic is observed with 45 bar rise at the model boundaries. They used closed boundary condition in the model that causes a global pressurizing in the medium. A

Table 1: The facies used in the SAIGUP geological modeling and their scales.

Facies name	**X Scale**	**Y Scale**	**Z Scale**
Offshore transition zone	0.5 m	0.5 m	0.5 cm
Lower shoreface	0.5 m	0.5 m	$0.5 - 2.0$ cm
Upper shoreface	0.5 m	0.5 m	$0.2 - 0.5$ cm
Coastal plane	75 m	-	-
Offshore	75 m	-	-
Channels	$0.04 - 1$ m	$0.04 - 1$ m	0.5 cm

local pressure rise above 60 bar is simulated near the injection well.

We use the SAIGUP geological realizations to study the pressure in large aquifers. However, the SAIGUP model size (9km $\times$ 3km $\times$ 80m) is considerably smaller than the extent of large aquifers. To compensate for the size, we consider open boundary conditions in the SAIGUP model by exaggerating the pore volume of the cells at the boundaries. This choice of boundary modeling results in an early relaxation of the pressure in the medium when the pressure pulse arrives at the boundary. Overall, the pressure values reported in our study are expected to be higher if they were modeled in a larger model.

This study complements [1, 2], in the sense that we herein analyze the sensitivity of pressure to the same geological parameters. In addition to the injection scenario used in [1, 2], we examine a different injection scenario with more realistic well control for the injection operation. A detailed study is given here for the pressure behavior during and after injection.

2 Geological parameters

In the SAIGUP geological modeling, six rock types were included to model a shallow-marine system. Each rock type was modeled at appropriate scales to honor the interaction of flow with various heterogeneity types at different spatial scales (Figure 1). Each facies was upscaled in a number of stages and finally all the rock types were mapped on a geological model with fine grid. Some of the meter-scale facies were modeled in three dimensions to capture anisotropy. Variation within each rock type was modeled either deterministically by considering a periodic pattern or modeled internally by stochastic population. Channels were modeled in fine grid and went through two stages of upscaling. Tests showed that when upscaled, various grid scale models produced similar results. The specifications of the rock types are given in Table 1. For more detail of the SAIGUP sedimentological modeling see [7].

The wave and fluvial depositional processes acting at the shoreline control the plan-view shape, the channel abundance in the delta plain and the abundance of mud-draped. These parameters were characterized within the SAIGUP modeling and varied in three levels that can be summarized as shorefaces. A wave-dominated deposition produces a straight plan-view shape, very few channels and no dipping barriers. If the river flux is high enough to dominate the wave system in the sea, a lobate shape shoreface generates with moderate numbers of channels and some dipping barriers. Higher levels of fluvial domination end up in two-lobe system with numerous channeling and dip barrier surfaces.

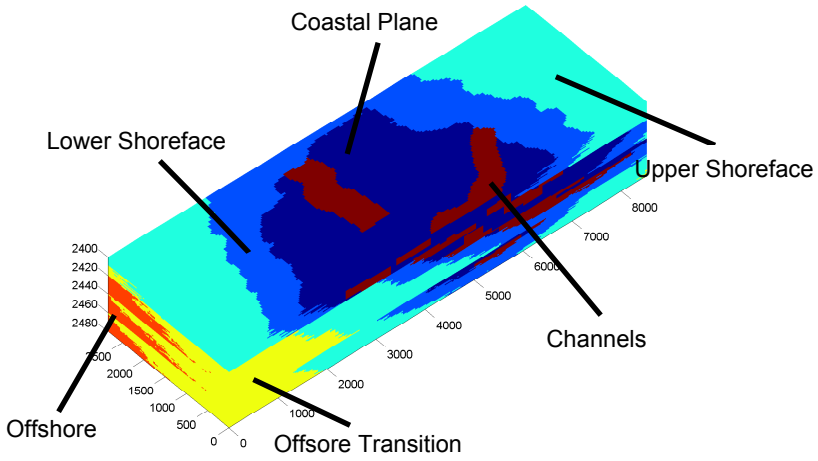

Figure 1: Geological modeling in the SAIGUP realizations contains six facies that represent a shallow-marine system.

Table 2: Geological modeling parameters

Parameter	**Value**
Model dimensions	3 km × 9 km × 80 m
Geological grid resolution	80 × 240 × 80
Simulation grid resolution	40 × 120 × 20
Simulation grid resolution	40 × 120 × 20
Average of lateral permeability	181 mD
Average of Vertical permeability	26.8 mD
Average of porosity	0.145

Table 3: Marker codes used in the result plots. The code level corresponds to levels in Figure 2.

Code	Description	Code level	Feature level
Thickness	Fault	thin/medium/thick	unfaulted/open/close
Shape	Lobosity	square/circle/diamond	flat/one-lobe/two-lobe
Size	Barriers	small/medium/large	10% / 50% / 90%
Color	Aggradation	blue/green/red	low/medium/high
Case no. counting	Progradation	first half/second half	up-dip / down-dip

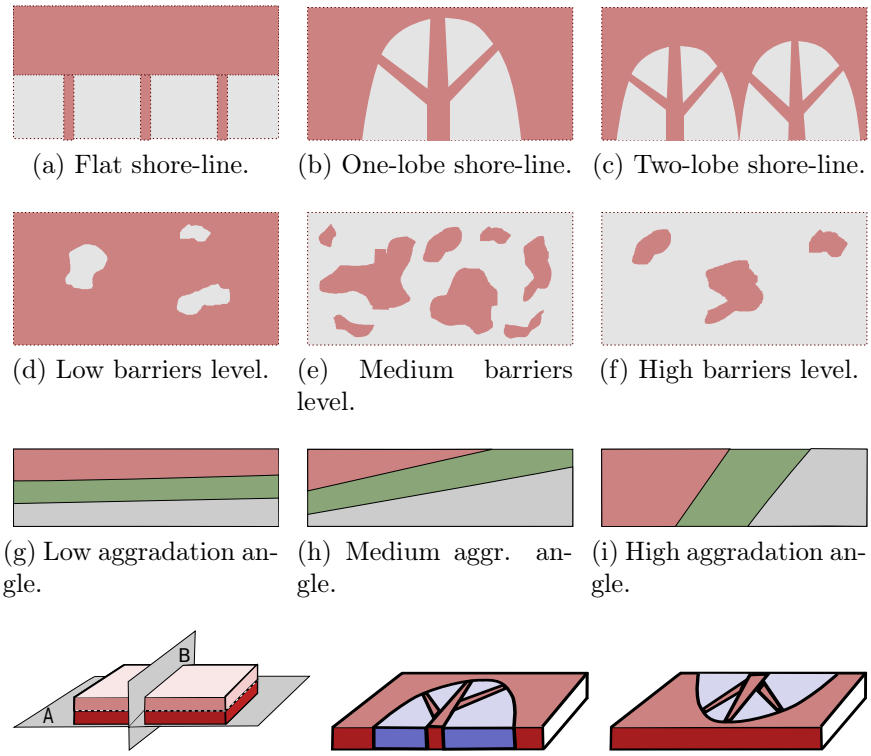

(a) Flat shore-line. (b) One-lobe shore-line. (c) Two-lobe shore-line.

(d) Low barriers level. (e) Medium barriers level. (f) High barriers level.

(g) Low aggradation angle. (h) Medium aggr. angle. (i) High aggradation angle.

(j) Slice A is used in Figures a-f and B in Figures g-i. (k) Updip progradation. (l) Downdip progradation.

Figure 2: The studied geological features. a-c) Shoreline shape, gray is for poor quality rock and brown color resembles a good quality rock. d-f) Barriers level defined by transmissibility multiplier. Gray color is for zero and brown color shows one. g-i) Aggradation angle. k-l) Progradation direction.

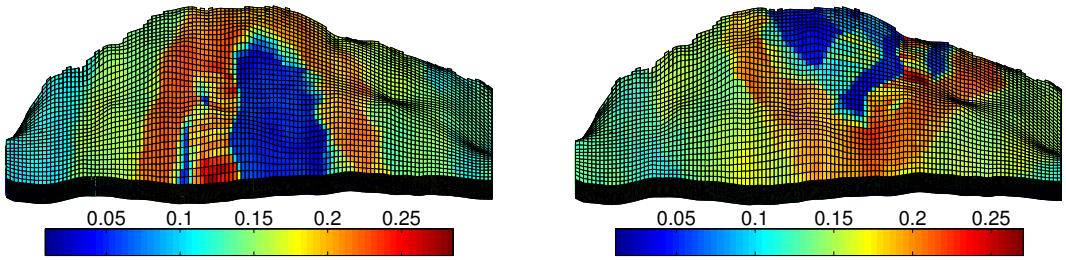

(a) Unfaulted grid.

(b) Faulted grid.

Figure 3: Porosity values shown for cases with up-dip (left) and down-dip (right) progradations.

Shale draped surfaces may provide both horizontal and vertical barriers to fluid flow and are common in fluvial-dominated systems. They are the product of very shortterm fluctuations in the fluvial systems and periodic floods in the delta. Shore line shape is correlated to the shape of these flow barriers; straight shorelines typically have planar seaward-dipping clinoforms and curved shorelines have clinoforms that resemble top-truncated cones. Within the SAIGUP modeling process, these barrier surfaces were modeled as stepped transmissibility multipliers on the cell faces. Dipping barriers were not included in the flat shoreline models and in the realizations with lobosity, between one and three barriers were included. For the purpose of SAIGUP, three levels of barrier coverage were modeled for all of the SAIGUP models (10%, 50% and 90% coverage), with a smaller subset of 12 models having 100% coverage. All levels of coverage were subsequently slightly modified by removing the barriers where the fluvial channel deposits were present, since clinoforms are a feature of the delta front and not formed within a channel setting.

Aggradation angle models the variation of shoreline in a 2D, depositional dip-orientated cross-section. Within the SAIGUP study, the trajectory vary between horizontal progradation and pure vertical aggradation. Aggradation angle is a function of the balance between sediment supply and the rate of accommodation in the sea. When the fluvial flux increases in level, the deposition from the river toward the sea pile toward the sea and make the aggradation angle.

The final factor varied during the sedimentological modeling was the progradation or depositional-dip direction. The progradation direction is important in the CO_2 injection operations because the structural dip controls the injection well position and the direction of CO_2 plume movement during Injection. In Figure 3, injecting in high permeablity channels enhances the well injectivity and lowers the pressure build-up in the medium.

The faults are modeled as post-depositional with no related changes in facies thickness or shoreline orientations. Faulting process causes layers with different quality to become adjacent (Figure fig:fltZ). This can enhance the pressure connectivity by breaking the sealing layers, or it can produce sealed compartments that are not connected to the rest of the domain.

We have selected five geological parameters from the SAIGUP project to study the impact of heterogeneity on the pressure responses in a typical CO_2 injection problem. The considered

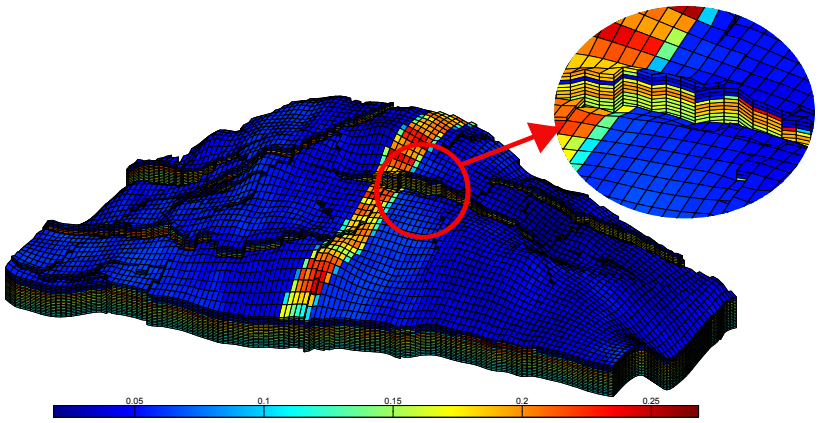

Figure 4: Faults connect layers with different rock types.

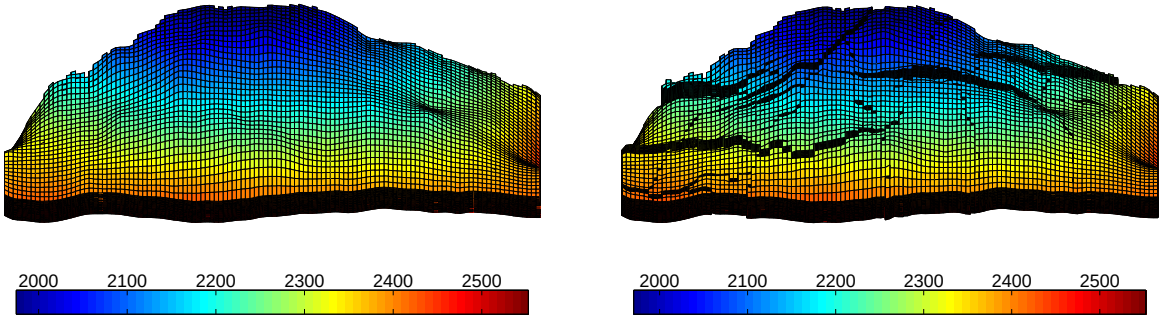

(a) Unfaulted grid.

(b) Faulted grid.

Figure 5: Models used in the study. Depth in meter is shown by color.

features with the grading levels in each one are shown in Figure 2. In addition to the features shown in Figure 2, we consider faulting levels: unfaulted, open, and close faults. Each of these features are represented with codes in the plots throughout the paper; such as shape, size, and color which are explained in Table 3.

In the last step, the produced geological realizations were upscaled via flow-based methods to a coarse grid that is suitable for detailed flow simulation. Detail of geological and simulation grid is given in Table 5.

3 Injection scenario

We assume open boundaries on the sides of the simulation model (Figure 6). The spatial dimensions of the model are relatively small (9km $\times$ 3km $\times$ 80m). Therefor, assuming closed or semi-closed boundaries results in an unrealistic pressure build-up in the domain due to

Table 4: Geological and simulation model specifications. Averaged values are arithmetic averages and belong to a selected geological model (shown in Figure 1).

Parameter	**Value**
Model dimensions	3 km × 9 km × 80 m
Geological grid resolution	$80 \times 240 \times 80$
Simulation grid resolution	$40 \times 120 \times 20$
Simulation grid resolution	$40 \times 120 \times 20$
Average of lateral permeability	181 mD
Average of Vertical permeability	26.8 mD
Average of porosity	0.145

the injection operation. The open boundaries are modeled by exaggerating the two last cells at the boundaries. The second last cell pore volume is magnified 10^3 times and the pore volume of cells at the boundary is multiplied by 10^6. These values are calculated such that no considerable pressure change occurs in the out-most cells at the boundary. No-flow boundary condition is applied on the top and bottom of the model. Moreover, the evaluated side on the crest is located at a large fault displacement and is considered as a close boundary.

We use one injection well in the model to study the medium response to the pressure imposed by the a single injection point. Also, it is easier to study the CO_2 plume evolution in a model with one injector. However, using only one injector does not describe the impact of well location in the model and the outcome of the study can be different if we choose a different location for the injector. We studied various locations in a homogeneous model to choose an injection point that allows a relatively long travel path for the injected CO_2. We inject in the flank and the injected CO_2 travels upward to the crest due to the buoyancy force. If the medium is homogeneous, following the injection we expect one big plume to be constructed and this plume to move up due to the gravity force until it accumulates under the structural trap beneath the cap rock. The well is opened to flow in the last four cells in the vertical direction, i.e., in the lowest layer of the model.

To reduce the effect of well location , one can inject through a number of wells distributed in the medium. To evaluate the impact of injection location and the interaction of the injector with the local heterogeneity, we can try the study for many simulations with different injection locations. This will dramatically increase the number of detailed flow simulations and it is not considered in this study.

Slightly compressible supercritical CO_2 is considered and we seek to inject a volume of 4×10^7 m^3, which amounts to 20% of the total pore volume of the models. After the injection period, early plume migration is simulated in all of the studied cases and the simulation ends at 100 years. We use Corey-type quadratic functions for relative permeability, with end points 0.2 and 0.8 in both phases.

In this study, two injection strategies are implemented. In the first strategy (which is similar to the one used in [1]), the entire CO_2 volume is injected within 30 years at a constant volumetric rate. In the second strategy, we set an operational pressure constraint on the injector and continue injecting with appropriate rates to keep the pressure within the limit. We do some pressure response calculations to see the propagation of pressure pulses

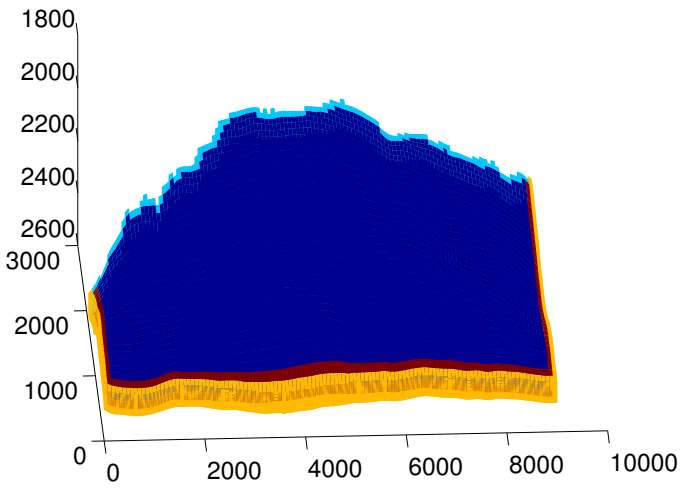

Figure 6: Boundaries in the flow simulation model; the crest boundary (light blue) is considered closed to flow. Cells' pore volume at other sides of the model are multiplied by 10^3 (red) and 10^6 (yellow) to model the open boundaries on the sides.

in the medium for both strategies.

In the pressure-constrained strategy, the injector operates with the priority of injecting a volumetric rate of 3650 m^3/day. A pressure constraint of 400 bar is set on the injector. If the well bottom-hole pressure goes higher than that, the well priority changes to continue operating at 400 bar by reducing the injection rate until the target CO_2 volume is injected into the medium. As soon as the total injected volume reaches this number, the injector will be shut from the bore-hole and no injection happens for the rest of simulation time.

4 Pressure analysis

We start by discussing the pressure responses we will use in our study for one particular realization. Then we do the full analysis by considering all of the 160 specified realizations, which are made by combining the geological variable levels discussed earlier[1]. Response plots are shown and discussed accordingly. Most of the reported results are chosen at 2.4 hours (0.1 day), i.e., at the beginning of injection. At that time, the system pressure response is higher compared to the later times when the pressure in the system drops to lower values (Figure 7b). In additon, at this time the same amount of CO_2 is injected in all cases, which allows for a fair comparison between cases.

Four types of responses are considered to be basis for the comparison between cases. One important question is how fast we can inject into a realization. To compare different cases, injection time is calculated considering a fixed total volume of injection in all models. Pressure behavior in the system is studied, by looking at aquifer average pressure and pressure elevation across the well. An overpressure region is defined in which the volumetric spread of over-pressurized locations in the model is measured. Finally, the farthest place from the

[1]Combining all the features and levels makes 162 cases. However, two cases were missing in the original data set.

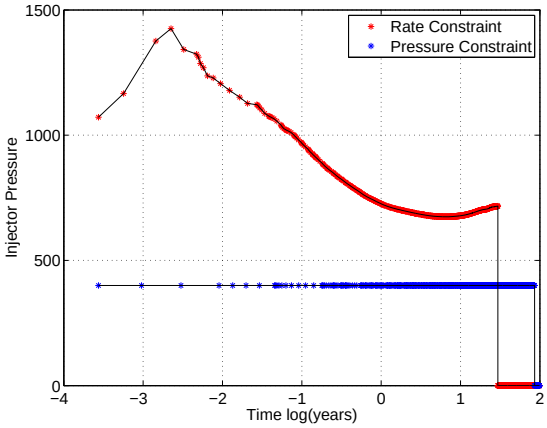

(a) Pressure in the injector versus logarithm of time.

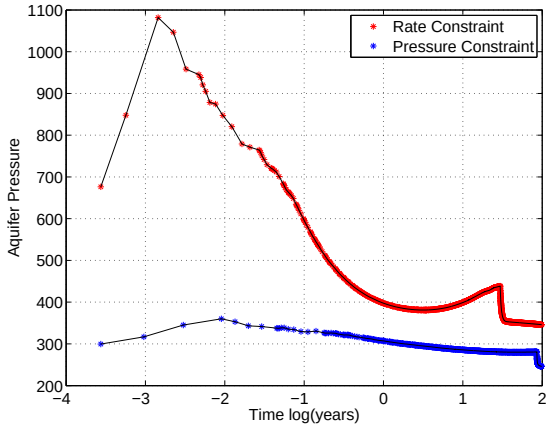

(b) Average aquifer pressure versus logarithm of time.

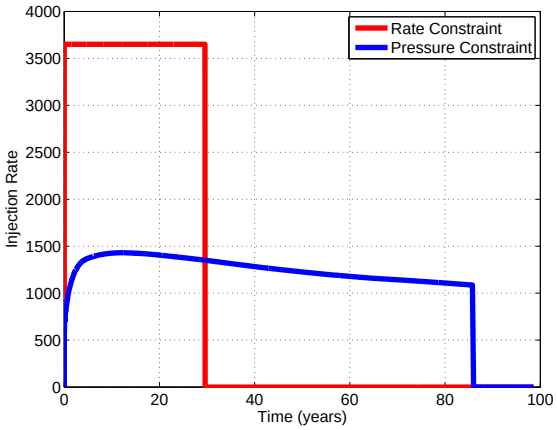

(c) Volumetric injection rate.

Figure 7: Aquifer and well pressure and injection rate in different injection scenarios shown for a test case.

Table 5: Simulation parameters used in the study.

Parameter	**Description**	**Value**
S_{rw}	Residual brine saturation	0.2
$S_{r_{CO_2}}$	Residual CO_2 saturation	0.2
$\mathrm{K}_{r_{CO_2}}$	CO_2 relative permeability	$(1 - S_{CO_2} - S_{rw})^2$
K_{rw}	Brine relative permeability	$(S_w - S_{r_{CO_2}})^2$
ρ_{CO_2}	CO_2 density at surface conditions	700 kg/m^3
ρ_w	Brine density at surface conditions	1000 kg/m^3
C_m	Medium compressibility	0.3×10^{-6} 1/bar
P_0	Reference pressure for compressibility	400 *bar*
μ_{CO_2}	CO_2 viscosity at surface conditions	0.04 cP
μ_w	Brine viscosity at surface conditions	0.4 cP
q	Target injcetion rate	3600 m^3/day
P_{cr}	Critical well pressure	400 bar

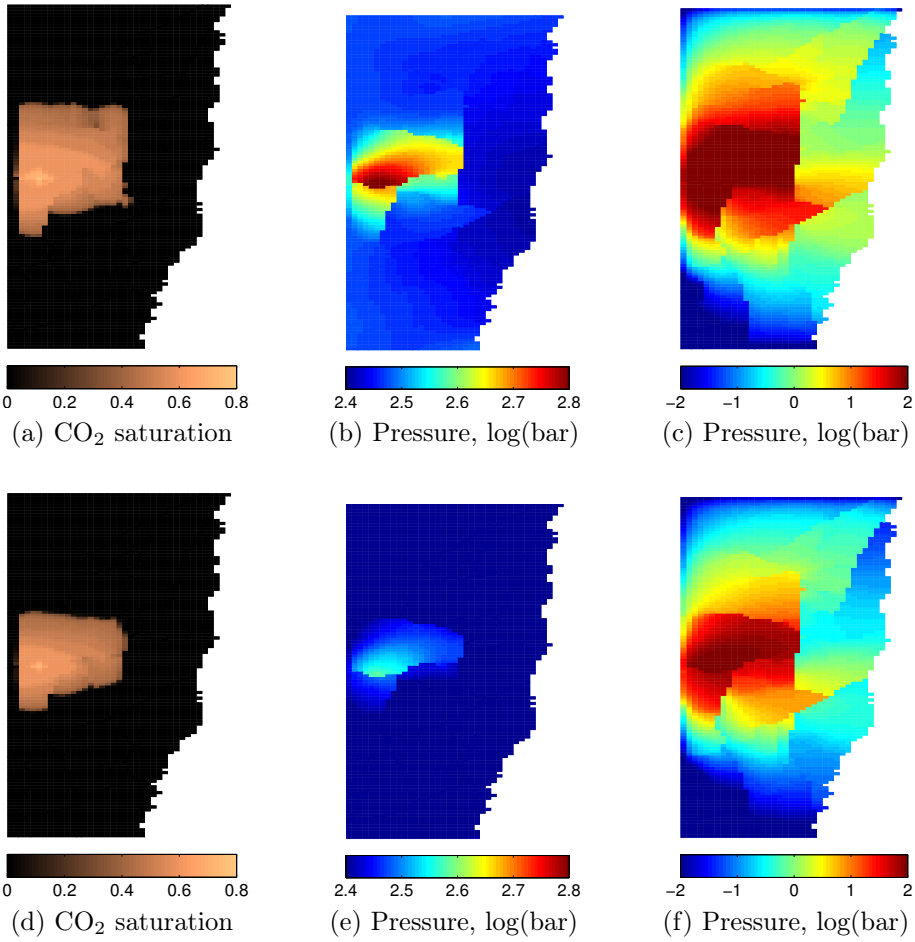

(a) CO_2 saturation (b) Pressure, log(bar) (c) Pressure, log(bar)

(d) CO_2 saturation (e) Pressure, log(bar) (f) Pressure, log(bar)

Figure 8: Responses at the middle of injection period (15 years). The first row corresponds to rate-constrained and the second row belongs to the pressure-constrained injection scenario. Figures c and f show the pressure build up from its initial value. Top view of last injection layer is shown in all figures.

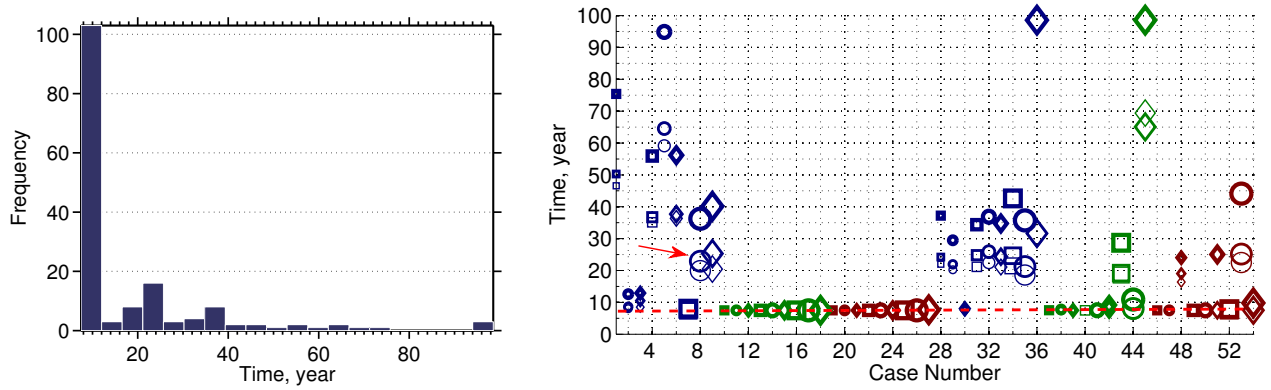

(a) Histogram of injection time in all cases.

(b) Case plot of injection time in all cases.

Figure 9: Time to inject quarter of the total specified CO_2 volume for all cases in the pressure-constrained scenario. The dashed red line in the right plot denotes the targeted injection time of 7.5 year, and the red arrow points to the case shown in Figure 8.

injection point that a pressure build up has reached is reported for each realization to see the impact of heterogeneity and channellings on how the pressure wave travels through the medium.

Figure 8 shows the pressure and saturation responses for the two injection scenarios in a selected case. This case has one lobe, parallel rock-type stratigraphy (i.e., low aggradation angle), and up-dip progradation. It is faulted with open faults and has high barrier level. Responses for the rate constrained scenario are given in Figures 8a, 8b and 8c, and those for the pressure constrained scenario are given in Figures 8d, 8e and 8f.

The pressure build-up in Figures 8c and 8f tells about heterogeneity impact on maintaining the pressure locally rather than transferring it across the medium. Comparing Figures 8b and 8c with Figures 8e and 8f, we see that imposing a pressure constraint on the injector significantly reduces the pressure build-up in the medium (as should be expected). However, the pressure disturbance propagates widely through the system in both cases (Figures 8c and 8f), far beyond the CO_2 invaded zones in Figures 8a and 8d.

4.1 Injection time

In the pressure-constrained scenario, the less the injectivity of the well is, the longer it will take to inject into the medium, keeping the pressure below the critical limit. In some of the cases it takes longer than 100 years (i.e., longer than the considered total simulation time) to inject the specified CO_2 volume. To compare cases, we therefore calculate the time at which a quarter of the objective volume is injected. In all cases, this amount is injected within the total simulation time.

Figure 9 shows the injection time for all cases, using the pressure-constrained scenario. For many cases, the injector keeps the target rate, and thus, it completes the injection in

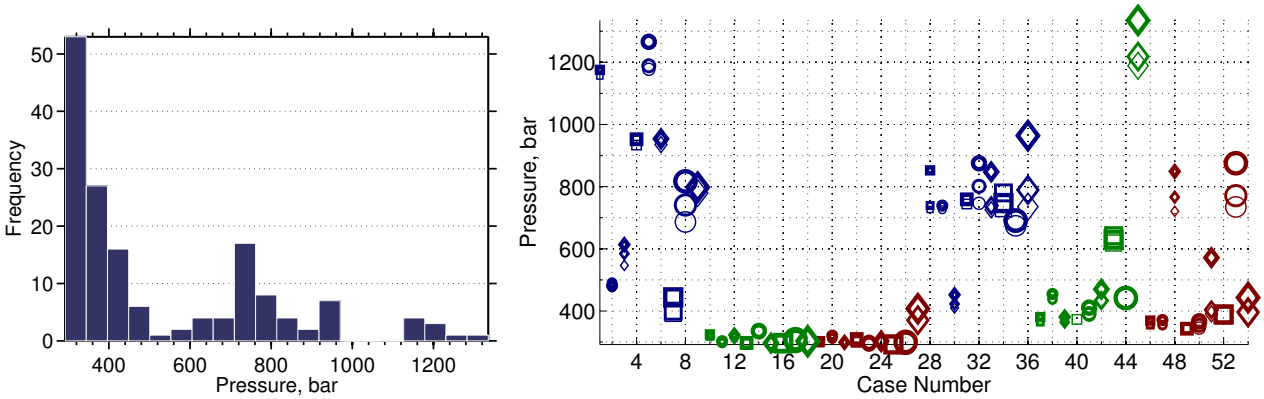

(a) Histogram of pressure values.

(b) Case plot of pressure values.

Figure 10: Average aquifer pressure for all cases in the rate-constrained scenario.

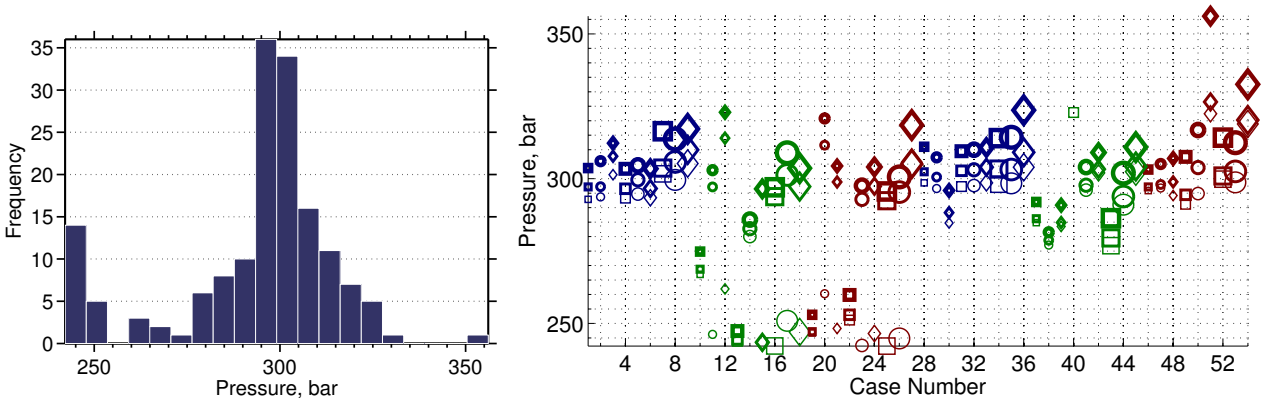

(a) Histogram of aquifer pressure values.

(b) Case plot of aquifer pressure values.

Figure 11: Aquifer average pressure for all cases in the pressure-constrained scenario.

7.5 years (the dotted red line in the figure). The rest of the cases require longer injection time, due to the lower injectivity of the medium. This leads to pressure control in the injector, followed by a decrease in the injection rate.

Different codes used in the plot of Figrure 9 are describe in Table 3. Most of the cases with lower injection rates in the plot are colored blue, which translates to a low aggradation angle. Also cases with closed faults, denoted by thick markers, have (significantly) longer injection time. Progradation effect is apparent on the higher aggradation cases: for some of the cases colored green and red in the second half of the plot in Figure 9, injection takes longer than the corresponding cases in the first half. Therefore, down-dip progradation, independent of aggradation angle level, can result in lower injectivity.

4.2 Well and aquifer pressure

To see the overpressure caused by different heterogeneities, we compare cases for their average pressure and well pressure elevation. Histograms of average aquifer pressure are shown in

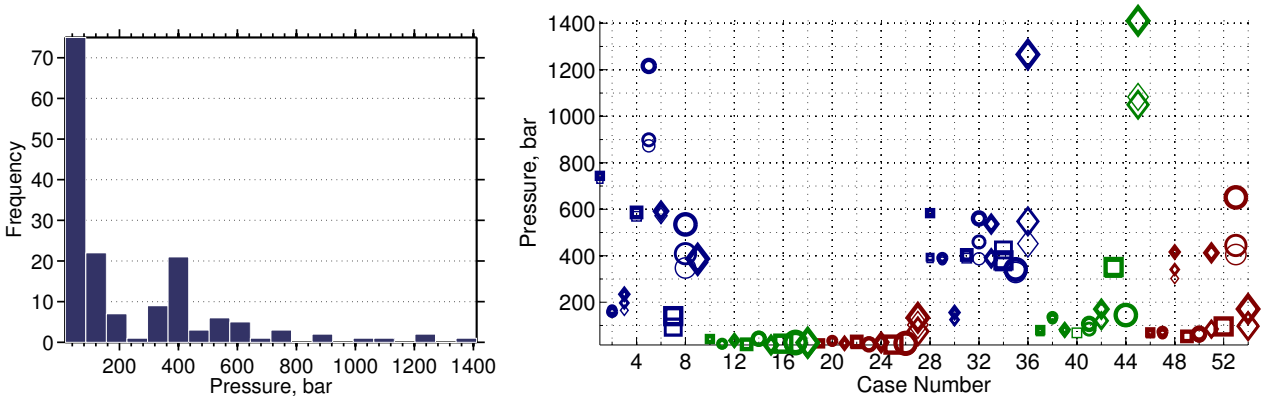

(a) Histogram of pressure elevation values.

(b) Case plot of pressure elevation values.

Figure 12: Average of injector pressure elevation for all cases in the rate-constrained scenario.

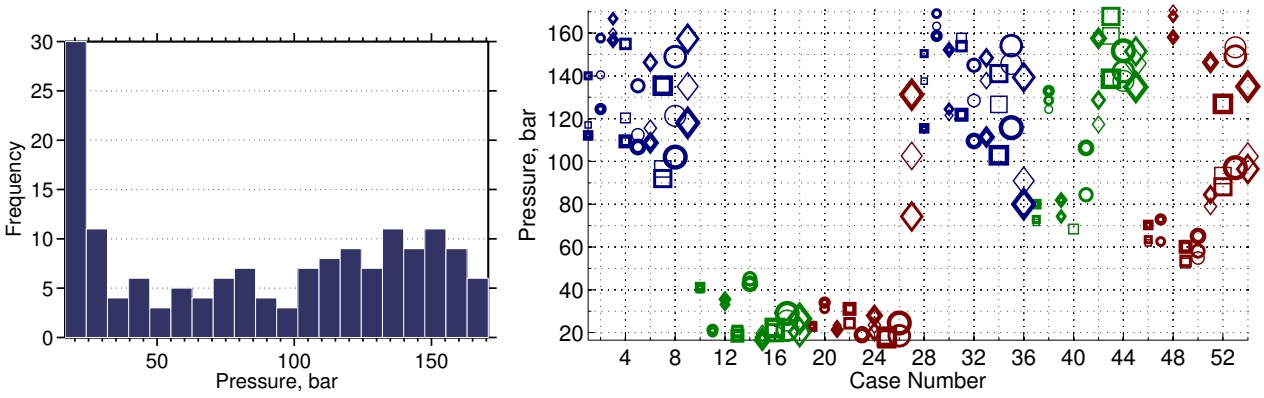

(a) Histogram of pressure elevation values.

(b) Case plot of pressure elevation values.

Figure 13: Average of injector pressure elevation for all cases in the pressure-constrained scenario.

Figures 10a and 11a for different injection scenarios and average aquifer pressure at 2.4 hours after the start of injection is plotted for all cases in Figures 10b and 11b. In the rate-constrained scenario, high ranges of average pressure are observed (Figure 10b). Effects of aggradation angle, progradation and faulting are visible in the plot. Three clusters can be identified in the histogram of Figure 10a with medium, high and extreme pressure values. In Figure 11a, a small group of cases show lower pressures, while most of cases are distributed around the mean value (which reads 300 bar).

We define the average well pressure elevation at time t_c as the temporal average of the difference between the bottom-hole pressure P_w and the average aquifer pressure $\bar{P}_a$:

$$\bar{\Delta P} = [\int_0^{t_c} (P_w - \bar{P}_a)\, \mathrm{d}t]/t_c. \tag{1}$$

Histograms of well pressure elevation values are shown in Figures 12a and 13a. Higher values imply a poor injectivity of the medium. We see in Figure 12 that maintaining the target rate will in many cases require a huge pressure elevation (up to 1400 bar in the worst cases) that would not be feasible nor possible to obtain. Pressure control on the injector reduces the range of pressure elevation variation below 170 bar. The average injector pressure elevation is plotted for all cases in Figures 12b and 13b.

Two regions can be identified in the medium, the region near the injection point; and the part of aquifer which is far from the injection point. The well-bore pressure is effected directly by heterogeneities in the near well-bore region, while the larger scale region influences the average aquifer pressure. Pressure elevation variations in Figures 12a and 12b are influenced by the heterogeneity near the well-bore, where the reaction to injecting a fixed amount of CO_2 starts by a local pressure build-up. Heterogeneity on the scale of aquifer plays a considerable role in the range of variations in Figures 13a and 13b. In the pressure-constrained scenario, local pressure is controlled by putting a constraint on the well. Hence, the pressure elevation variations are controlled by the average aquifer pressure.

As we see in Figure 12b, low aggradation angle and down-dip progradations result in a poor injectivity and high pressure buildup in the injector. Vertical transmissibility drops dramatically for low aggradation angles [1]. This restricts the pressure transfer within the injection layer, and therefore the pressure builds up locally around the well. Moreover, in cases with down-dip progradation the low permeabilty rocks surrounding river branches near the injector result in a local pressure buildup.

A group of cases in Figure 13 have a relatively low pressure elevation of less than 50 bar. These cases have a good injection quality, and the pressure is released through open boundaries easier than other cases. The rest of the cases show higher pressure elevation because of the heterogeneities in the larger scale, far from the injector. These results are obtained for a fixed injection location to examine the geological uncertainty impact on injectivity. In practice, the injector must be drilled and completed in the best formation with highest possible injectivity.

Faults influence both local pressure build-up near the injector as well as the average aquifer pressure. Therefore, they have a visible trend in many cases in Figures 12b and 13b (for example, see the three cases denoted by red circles in the right end of Figure 12b). This is specially more apparent in cases with high level of barriers.

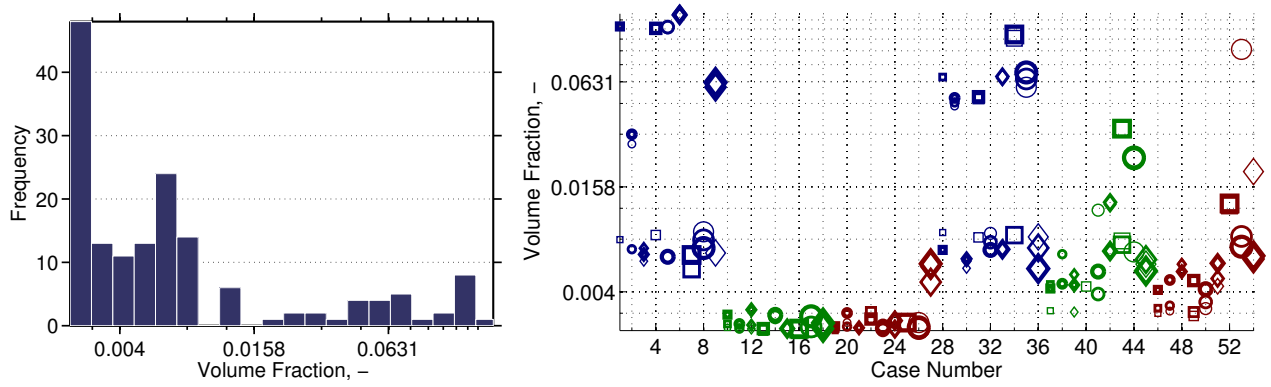

(a) Histogram of pressurized volume fractions.

(b) Case plot of pressurized volume fractions.

Figure 14: Pressurized volume fraction for all cases in the rate-constrained scenario.

4.3 Pressurized region

Here, we study the overpressure distribution in the medium. An absolute pressure limit of 300 bar is set as threshold, such that all cells with a pressure higher than this value form a region that is called the pressurized region. The volumetric fraction of this region is defined by the ratio of pressurized volume to the total volume of all active cells in the model.

Histogram and case plot of the pressurized volume fraction at the start of injection are given in Figure 14. Here, we clearly see that low agrradation angle is very influential in the pressure buildup in the injection zone. A group of cases with low aggradation angle have a relatively large pressurized region in Figure 14b. However, there are number of cases with low aggradation angle in Figure 14b that have a relatively low pressurized fraction. In these cases, the medium is conductive toward the open boundaries and the heterogeneity in the medium does not cause a major pressure buildup. Other observation in Figure 14b is the progradation effect; down-dip progradation, shows a rise in pressurized fraction for higher aggradation angles.

4.4 Build-up region

To study the pressure change, and how a pressure disturbance spreads through the medium, we use another metric. We calculate the pressure change by subtracting the initial hydrostatic pressure at each location from the current pressure. Different realizations are compared for the size of a region, which we call the buildup region, where the pressure increases from its initial value by 10 bar. The value 10 bar is chosen to make sure that the region has not reached the boundaries in any of the studied cases. The smaller the buildup region is, the less volume will be exposed to pressure change in the aquifer (Figure 15).

Higher pressure in the medium will obviously cause a larger buildup region. Impact of progradation on the pressure build-up is illustrated in Figure 15b. Up-dip progradation shows a relatively lower pressure buildup compared to down-dip progradation cases. We also see that aggradation dominates this effect, where cases with low aggradation angle show the same build-up pressure for both types of progradation directions (Note the blue colored markers

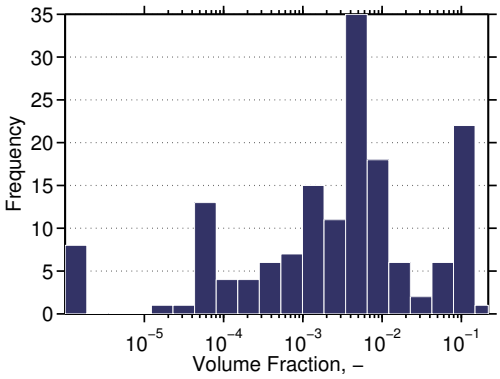

(a) Histogram of build-up volume fractions.

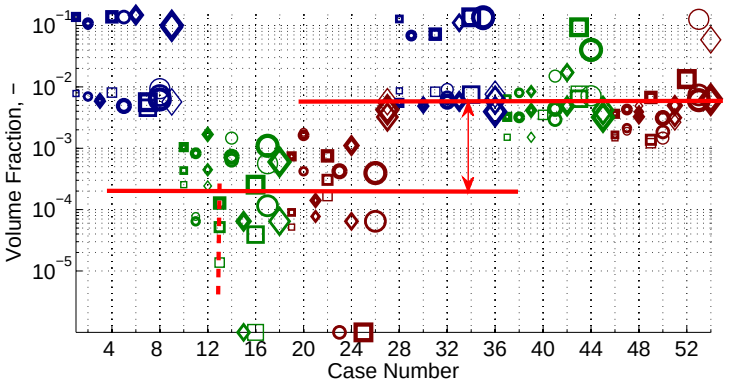

(b) Case plot of build-up volume fractions.

Figure 15: Build-up volume fraction for all cases in the rate-constrained scenario.

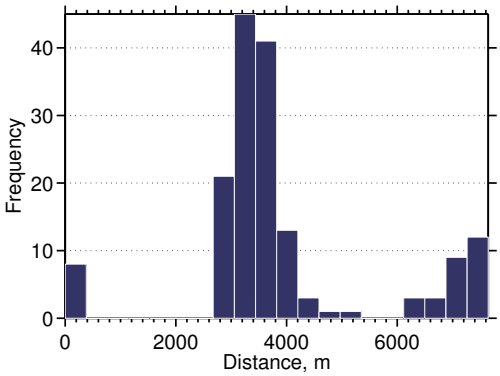

(a) Rate-constrained scenario.

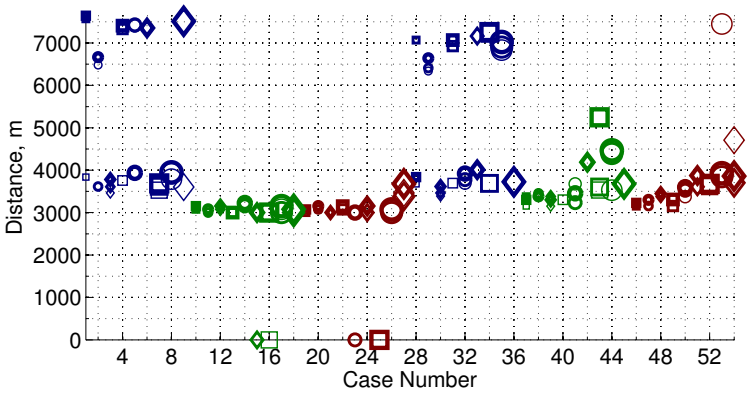

(b) Rate-constrained scenario.

Figure 16: The farthest pulse of the pressure build-up distance from the injection point for all cases in the rate-constrained scenario.

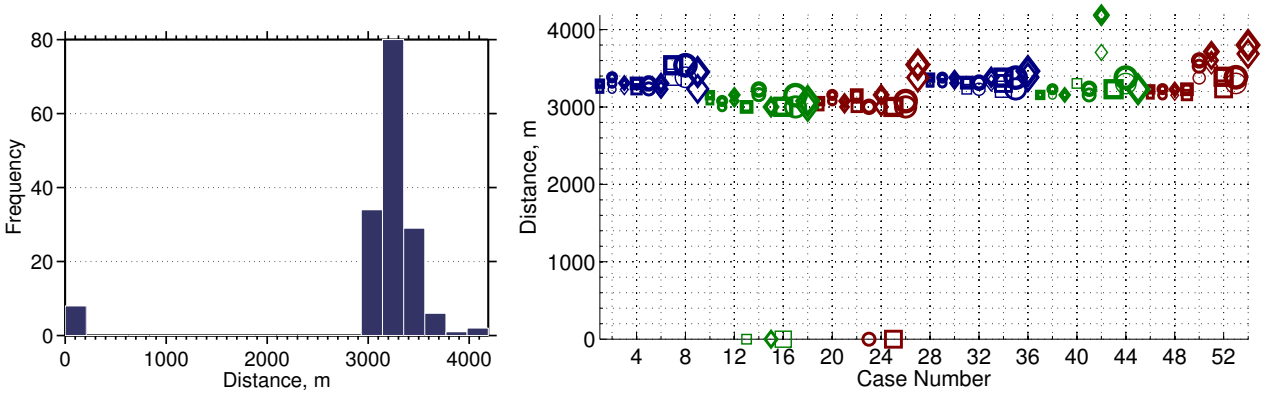

(a) Pressure-constrained scenario.

(b) Pressure-constrained scenario.

Figure 17: The farthest pulse of the pressure build-up distance from the injection point for all cases in the pressure-constrained scenario.

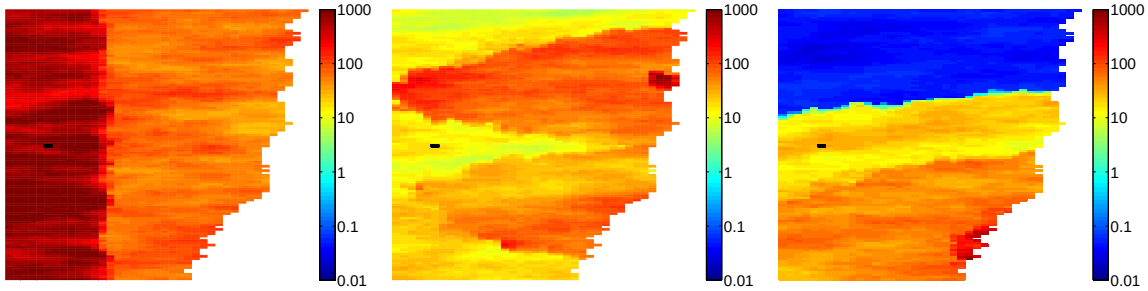

(a) (b) (c)

Figure 18: Permeability of three cases in unit millidarcies shown in color, and the Well location is illustrated with black color on each plot . Top view is shown in the plots.

that dont follow the lines in Figure 15b).

Several cases in Figure 15b show a trend for the fault parameter. The dashed line in the figure shows the trend of build-up pressure increase due to fault feature variations in three cases. Faulting changes the geometry of layers and puts different layers adjacent to each other. This enhances the connectivity in the medium. Local heterogeneities and closed faults around the injector make a larger build-up region, because they cause higher pressure build-up in the domain. In these cases, the effect of heterogeneity of different scales, namely on the scale of near injector and far from injector, are combined causing a larger buildup fraction.

4.5 Farthest pulse

As discussed earlier, irregular geometries like faults and unconformities can lead to pressure spread in the domain. Looking at the volume fraction of pressurized and buildup regions helps in comparing cases for their pressure conductivity, but it does not show the extent of pressure spread in the medium. For that reason, we also look at the farthest cell from the

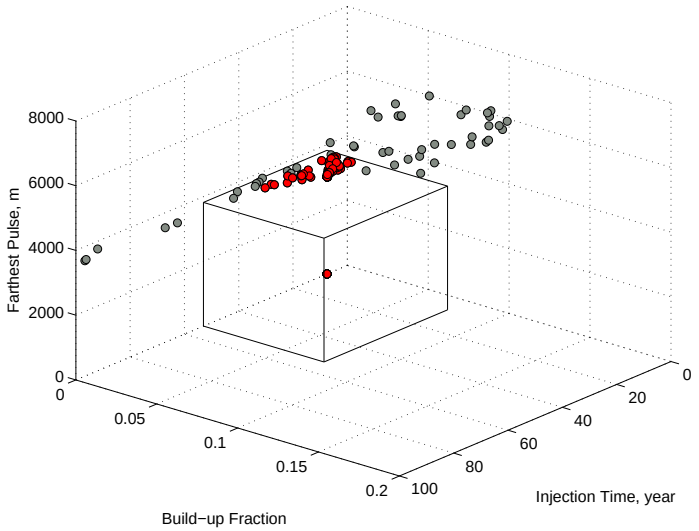

Figure 19: Pressure criteria implemented to filter the acceptable cases. Cases below the critical limits are plotted in red and cases exceeding the limits are plotted in gray.

injection point that falls within the buildup region defined earlier.

Figures 16 and 17 show the farthest pressure build-up distances from the injector in different injection scenarios. In Figure 16a, three groups of cases can be identified: cases with zero distance of farthest pressure build-up pulse, cases with medium distances, and those with large distances from the injection point. Three specific cases are chosen as samples from each of the groups. In the first group, the pressure does not exceed the 10 bar threshold from its initial value in the medium. For these cases, the injector is placed in a permeable region and the medium is conductive towards open boundaries (Figure 18a). Hence, the imposed injection pressure does not build up, neither locally around the well nor globally in the aquifer scale. The second group in Figure 16a have a medium range of $3 - 4$ km of distances from the injection point. Heterogeneity in these cases is not making a high pressure build-up around the injector and throughout the medium (Figure 18b).

In the third group, low permeability rocks in the injection layer cause a high pressure build-up around the injection point. If the injector zone is isolated by sealing heterogeneities, the pressure rises in a limited region. However, if the well is connected throughout the medium, and the heterogeneities in the aquifer scale contain relativly low permeability rocks, the pressure build up spreads wider in the aquifer. In Figure 18c, the injection point is located close to a low transmissibility rock. This rises the pressure level in the injector. Other parts of the aquifer are connected with poor quality rocks, resulting in a wide build-up region.

The farthest pulse distance ranges from 8 km to about 10 km in the extreme cases. By controlling the injection pressure, the maximum shrinks to less than 5 km (Figure 17a).

5 Discussion

So far, we reported the model responses that measure the pressure rise and pressure disturbance propagation in the domain. The pressurized volume fraction indicates the actual high

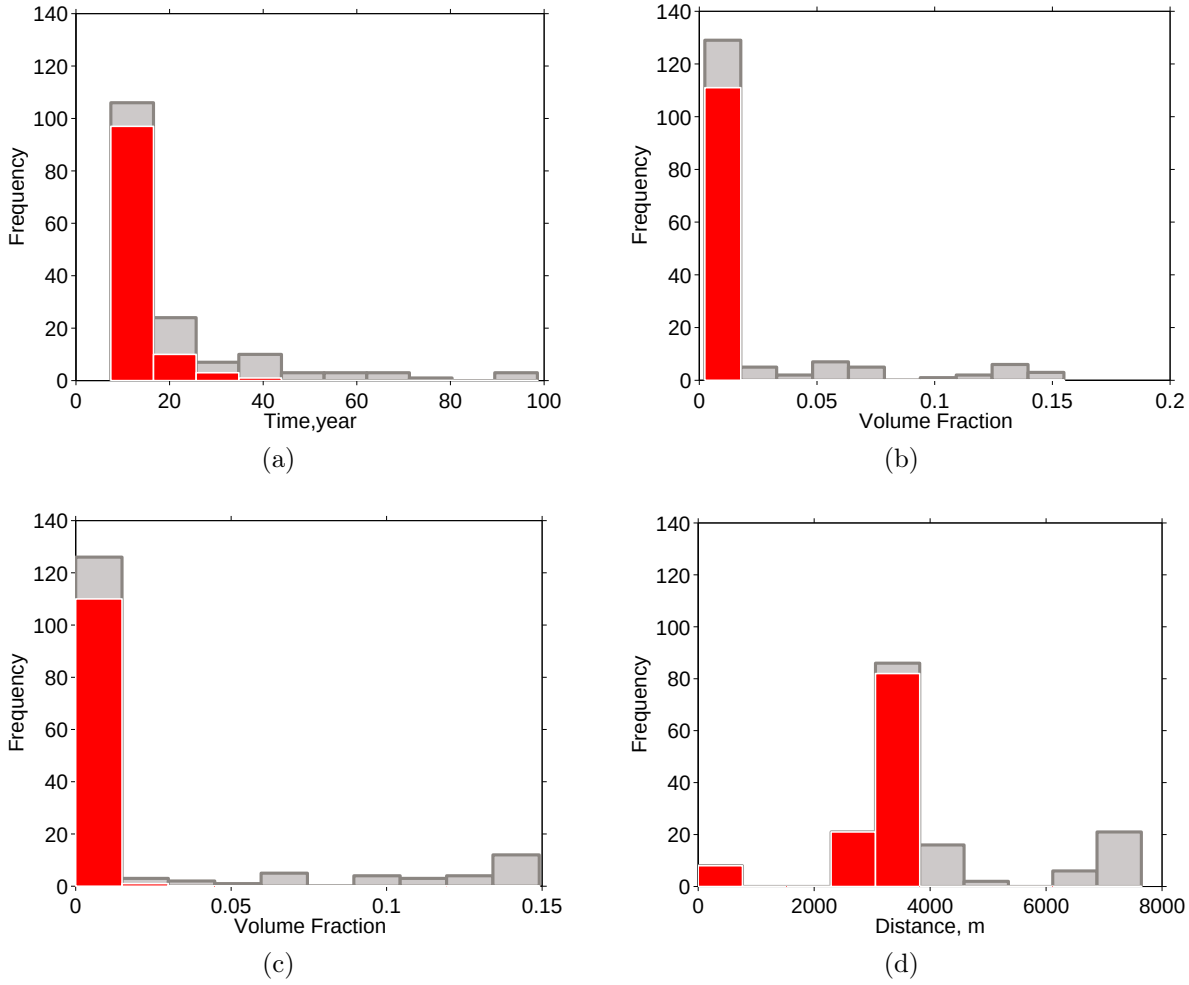

Figure 20: The histogram of filtered cases (red) compared with the histogram of all cases for different pressure responses: a) Injection time, b) pressurised volume fraction, c) build-up volume fraction, and d) farthest pulse distance from the injection point.

pressures that may occur in an injection operation. The build-up volume fraction and the farthest pulse are indicators of how the pressure disturbance is spread in the system. We are interested in limiting both the pressure increase and the area of the well pressure influence in the aquifer.

In most of the results, aggradation angle, progradation direction, and faults play a major role in the pressure behavior. For low aggradation angles, geological layers are made of rock types piled in a parallel stratigraphy. Thus, efficient vertical permeability is the harmonic average of these layers. If any of these layers contain a low-permeability rock, this fact will result in a low vertical permeability. Injecting into a limited space sealed vertically increases the pressure in the injection point.

The progradation direction can dominate the pressure behavior. It is very important to locate the injector in a high permeability zone that is connected to other parts of the domain via permeable channels. Injecting into the riverside of a shallow marine depositional system may result in locating the injection point in low-quality rock between river branches joining the sea. This fact increases the pressure significantly near the injection point and can result in a high well-bore and aquifer pressure.

Structural deformations due to faulting process can increase the connectivity in the medium. If the transmissibity in the aquifer scale is high, the injection pressure releases through the open boundaries. However, if the injection area is surrounded by low-quality medium, the pressure increases in the aquifer and the connectivity enhanced by the fault geometries spreads the build-up region in the domain. On the other hand, sealing faults results in high pressures within closed zones around the injection point. However, sealing faults may limit the pressure disturbance propagation in the domain.

From an operational perspective, pressure limits must be set to keep the operations within safe margins. One approach to study the safety of an operation could be setting critical limits on the pressure responses measured here. This limit is used to filter cases with desirable/acceptable pressure behaviors. The critical margins are inferred from the realistic operational requirments. In our pracice, we assume these margins to be 53 years for the injection time, 0.0787 for the pressurised volume fraction, 0.0745 for the build-up volume fraction, and 3822 m for the farthest pulse distance from the injection point. These values are selected from the mid points of range of variations in the results. By these assumptions, 49 cases out of total number of 160 cases exceed the critical limits.

Figure 19 shows the cases filtered by the pressure criteria. In Figure 19, the pressurized volume fraction is also considered in the filtration, although it is not shown in the plot axes. The plot shows that most of the cases that pass the filtering are concentrated in a region of low build-up fraction values. Figure 20 shows the histogram of filterd cases compared with the histogram of all studied cases for each response.

6 Conclusions

This work is a part of comprehensive sensitivity studies to assess the impact of geological heterogeneity on CO_2 injection and early migration. The aim of this study is to define preventing measures that can be used to avoid high pressures and the damages that accompanied them during the injection operations. Simulation responses related to the pressure behavior in

the system are defined and calculated for two CO_2 injection scenarios. Geological variations in shallow marine depositional systems are examined by using large number of realizations representing a spectrum of sedimentological and structural parameters. Operational critical values are considered for the defined preventive measures.

Most of the studied responses show a higher relative sensitivity to aggradation, progradation, and faulting. Low aggradation angles keep the flow restricted in a limited space. In cases with low rock quality in injection layers, pressure builds up in the well-bore. Injecting in down dip progradation normally ends up in a higher pressure build-up and a lower injectivity. In the down dip progradation, the majority of the region around injection point is made of low quality rock. Faults change the geometrical structure of the medium and they put different layers in contact. Pressure disturbances can leak through faults to larger distances from the injection point. Closed faults can significantly reduce the injectivity quality.

The workflow of the pressure study demonstrated here can be used in specific studies in the context of geological uncertainty. The workflow can be used for other depositional systems and different values for operational limits can be used, which might lead to outcomes different than the results reported here.

References

[1] M. Ashraf, K.A. Lie, Nilsen, and A. Skorstad. Impact of geological heterogeneity on early-stage CO_2 plume migration: Sensitivity analysis. In *ready for submission*, 2012.

[2] M. Ashraf, K.A. Lie, H.M. Nilsen, J.M. Nordbotten, and A. Skorstad. Impact of geological heterogeneity on early-stage CO_2 plume migration. In *CMWR*, 2010.

[3] Jens Birkholzer, Quanlin Zhou, Jonny Rutqvist, Preston Jordan, Keni Zhang, and Chin-Fu Tsang. Research project on co2 geological storage and groundwater resources: Large-scale hydrological evaluation and modeling of impact on groundwater systems. 2008.

[4] B. Cailly, P. Le Thiez, P. Egermann, A. Audibert, S. Vidal-Gilbert, and X. Longaygue. Geological storage of CO_2: A state-of-the-art of injection processes and technologies. *Oil & Gas Science and Technology*, 60(3):517–525, 2005.

[5] A. Cavanagh and N. Wildgust. Pressurization and brine displacement issues for deep saline formation CO_2 storage. *Energy Procedia*, 4:4814–4821, 2011.

[6] Ethan R Chabora and Sally M Benson. Brine displacement and leakage detection using pressure measurements in aquifers overlying co< sub> 2</sub> storage reservoirs. *Energy Procedia*, 1(1):2405–2412, 2009.

[7] J.A. Howell, A. Skorstad, A. MacDonald, A. Fordham, S. Flint, B. Fjellvoll, and T. Manzocchi. Sedimentological parameterization of shallow-marine reservoirs. *Petroleum Geoscience*, 14(1):17–34, 2008.

[8] T. Le Guenan and J. Rohmer. Corrective measures based on pressure control strategies for CO_2 geological storage in deep aquifers. *International Journal of Greenhouse Gas Control*, 2010.

[9] T. Manzocchi, J.N. Carter, A. Skorstad, B. Fjellvoll, K.D. Stephen, JA Howell, J.D. Matthews, J.J. Walsh, M. Nepveu, C. Bos, et al. Sensitivity of the impact of geological uncertainty on production from faulted and unfaulted shallow-marine oil reservoirs: objectives and methods. *Petroleum Geoscience*, 14(1):3–11, 2008.

[10] J.D. Matthews, J.N. Carter, K.D. Stephen, R.W. Zimmerman, A. Skorstad, T. Manzocchi, and J.A. Howell. Assessing the effect of geological uncertainty on recovery estimates in shallow-marine reservoirs: the application of reservoir engineering to the SAIGUP project. *Petroleum Geoscience*, 14(1):35–44, 2008.

[11] Shlomo P Neuman and Paul A Witherspoon. Theory of flow in a confined two aquifer system. *Water Resources Research*, 5(4):803–816, 1969.

[12] J.P. Nicot. Evaluation of large-scale CO_2 storage on fresh-water sections of aquifers: an example from the Texas Gulf Coast Basin. *International Journal of Greenhouse Gas Control*, 2(4):582–593, 2008.

[13] J. Rutqvist, J. Birkholzer, F. Cappa, and C.-F. Tsang. Estimating maximum sustainable injection pressure during geological sequestration of CO_2 using coupled fluid flow and geomechanical fault-slip analysis. *Energy Conversion and Management*, 48(6):1798–1807, 2007.

[14] J. Rutqvist and C.F. Tsang. A study of caprock hydromechanical changes associated with CO_2 injection into a brine formation. *Environmental Geology*, 42:296–305, 2002. 10.1007/s00254-001-0499-2.

[15] Solomon Susan. *Climate change 2007-the physical science basis: Working group I contribution to the fourth assessment report of the IPCC*, volume 4. Cambridge University Press, 2007.

[16] L.G.H. van der Meer. Investigations regarding the storage of carbon dioxide in aquifers in the Netherlands. *Energy Conversion and Management*, 33(5-8):611–618, 1992.

[17] L.G.H. van der Meer. The conditions limiting CO_2 storage in aquifers. *Energy Conversion and Management*, 34(9-11):959–966, 1993.